

Lepton Flavor Violation in Supersymmetric SO(10) Grand Unified Models

Xiao-Jun Bi, Yuan-Ben Dai, and Xiao-Yuan Qi

*Institute of Theoretical Physics, Academia Sinica,
P.O. Box 2735, Beijing 100080, People's Republic of China*

Abstract

The study for lepton flavor violation combined with the neutrino oscillation may provide more information about the lepton flavor structure of the grand unified theory. In this paper, we study two lepton flavor violation processes , $\tau \rightarrow \mu\gamma$ and $Z \rightarrow \tau\mu$, in the context of supersymmetric SO(10) grand unified models. We find the two processes are both of phenomenological interest. In particular the latter may be important in some supersymmetric parameter space where the former is suppressed. Thus, Z-dacay may offer another chance for looking for lepton flavor violation.

I. INTRODUCTION

Super-Kamiokande data on the atmospheric neutrino anomaly presents a strong evidence for the existence of neutrino oscillations. The anomaly can be explained by $\nu_\mu - \nu_\tau$ oscillation

with $\delta m_{23}^2 = (1 - 8) \times 10^{-3} eV^2$ and a large mixing angle $\sin^2(2\theta_{\mu\tau}) = 0.8 - 1$ [1,2]. In addition, the long standing solar neutrino deficit can also be interpreted as another type of neutrino oscillations [3,4]. Assuming that the LSND anomaly [5] will finally disappear all these observations about neutrinos can be accommodated in a model with three very light active left-handed neutrinos. Many such models have been proposed to explain the measured neutrino parameters since Super-Kamiokande first published the data [6]. Among them a natural explanation of the neutrino masses is provided by grand unified models which interpret the very light neutrino masses compared with the quarks and charged leptons by the see-saw mechanism [7]. Especially in SO(10) grand unified models, in which the right-handed (RH) neutrinos have masses of the order about unification scale and the lepton masses and the quark masses are related, correct neutrino masses can be obtained [8]. The measured neutrino masses are even regarded as a new evidence supporting the grand unification idea [9]. As been argued in Ref. [8] a value for $m(\nu_\tau) \sim \frac{1}{20} eV$ falls into a natural range predicted by a grand unified model based on either a string-unified G(224) model or a SO(10) grand unified model. Furthermore, grand unified theory (GUT) has the advantage that it relates the neutrino problem, its masses and mixings, with charged lepton and quark masses and mixings into a large fermion flavor problem and thus gives more definite predictions.

Conversely, the parameters measured in the neutrino sector can provide a window on the grand unified theory study and they also give important feedback on the problems of quarks and charged lepton masses as they are all related in the GUT. A direct inference of neutrinos being massive is the existence of a Kabayashi-Maskawa like matrix for the lepton sector. However, the processes violating lepton flavors due to this matrix is too small to be observed because of the tiny neutrino masses. In the supersymmetric GUTs the high energy lepton flavor violation (LFV) interactions may leave trace in the mass matrices of scalar partners of leptons by renormalization effects, which drives low energy LFV processes since the mass matrix of the charged leptons and that of sleptons can not be diagonalized

simultaneously. Therefore, the study of the LFV process may provide important information on the flavor structure of the supersymmetric GUTs. Various LFV processes have been studied in different theoretical frameworks by a number of authors [10–14].

There are two purposes of this work. One is to study the LFV processes in the context of supersymmetric SO(10) grand unified models with a “lopsided” texture for the mass matrices of the down quark and charged lepton which has been advocated by a number of authors to accommodate the large $\nu_\mu - \nu_\tau$ mixing and small V_{cb} [15,16,8]. If the experimental sensitivity on $\tau \rightarrow \mu\gamma$ can reach down to 1×10^{-9} [10], not only this process can be observed but it can even be used to discriminate different fermion textures in the grand unified models. Another purpose of this work is to present the analytic formulas for the branching ratio of the process $Z \rightarrow \tau\mu$ in the minimal supersymmetric standard model (MSSM) and the numerical study in the class of models considered by us. This calculation seems absent in the literature. This calculation is triggered by the Giga-Z option of the Tesla project which may expect the 10^9 Z bosons at resonance [17]. The upper limit for the branching ratios could be improved down to $BR(Z \rightarrow \mu^\pm \tau^\mp) < f \times 2.2 \times 10^{-8}$ with $f = 0.2 \sim 1$. We find this process is quite interesting phenomenologically since in some supersymmetric parameter space $\tau \rightarrow \mu\gamma$ being suppressed, this process can be important however.

The paper is arranged as follows. In sec II we discuss the origin of the LFV interactions in a supersymmetric grand unified model and the Renormalization Group Equations(RGE). In sec III we present the formulas for the branching ratios of the two processes. In Sec IV we briefly introduce a grand unified model proposed in Ref [15] that we used in our calculations. The numerical results are presented in Sec V and we summarize and give conclusions in Sec VI.

II. RENORMALIZATION GROUP EQUATIONS AND LOW ENERGY SUPERSYMMETRIC SPECTRUM

A. Origin of Lepton Flavor Violation

If the SM is extended with massive and non-degenerate neutrinos, LFV processes may be induced. However, such processes are highly suppressed due to the smallness of the neutrino masses. The branching ratio is proportional to $\delta m_\nu^2/M_W^2$ which is hopeless to be observed [18]. When supersymmetry enters the theory the scene changes completely. The LFV may also be induced through the generation mixing of the supersymmetric soft breaking terms of the lepton sector. However, arbitrary mixing of these soft terms in the MSSM are not predictive. In our calculations we adopt the supergravity mediated supersymmetry breaking mechanism to produce universal soft terms at the GUT scale M_{GUT} , because non-universal soft terms at M_{GUT} may produce too large low energy LFV observable effects [10,11]. The tree level universal soft terms may induce non-diagonal terms at low energy by radiative corrections including LFV interactions at high scale. Our procedure includes calculating the low energy supersymmetric soft terms which is not generation universal now by integrating the RGEs and then calculate the LFV branching ratios induced by these non-universal soft terms.

For a supersymmetric SO(10) grand unified model, the structure below M_{GUT} where the grand unification has been spontaneously broken is the same as the MSSM supplemented with MSSM singlet RH neutrino superfields. The superpotential of the lepton sector is now

$$W = f_\nu^{ij} \hat{H}_2 \hat{L}_i \hat{N}_j + f_l^{ij} \hat{H}_1 \hat{L}_i \hat{E}_j + \frac{1}{2} M^{ij} \hat{N}_i \hat{N}_j + \mu \hat{H}_1 \hat{H}_2 \quad (2.1)$$

where f_ν and f_l are the Yukawa coupling matrices, M is the RH neutrino mass matrix. i, j are the generation indices. Anti-symmetric tensor ϵ^{ab} is implicit to contract the SU(2)

doublets with $\epsilon^{12} = -1$. In general, f_ν and f_l can not be diagonalized simultaneously, which is the origin of LFV interactions. Diagonalize f_ν and f_l by bi-unitary rotations,

$$\begin{aligned} f_l^\delta &= U_L^\dagger f_l U_R \\ f_\nu^\delta &= V_L^\dagger f_\nu V_R \end{aligned} \quad (2.2)$$

where $U_{L,R}$, $V_{L,R}$ are all unitary matrices. Then define

$$V_D = U_L^\dagger V_L \quad (2.3)$$

which is analog to the KM matrix V_{KM} in the quark sector. V_D is crucial for LFV processes. The RH neutrino masses are not much lower in order compared to M_{GUT} in SO(10) grand unified models. After the RH neutrinos are decoupled and H_2 gets VEV v_2 of weak scale we get three light left-handed (LH) Majorana neutrinos with mass matrix $m_\nu = -(f_\nu v_2) M^{-1} (f_\nu v_2)^T$ by see-saw mechanism. Suppose $m_\nu m_\nu^\dagger$ is diagonalized by V_L^ν , then the matrix

$$V^{MNS} = U_L^\dagger V_L^\nu \quad (2.4)$$

determines the neutrino oscillation parameters. In the published grand unified models which emphasize the neutrino oscillations the large $\nu_\mu - \nu_\tau$ mixing angle in V^{MNS} is mainly coming from U_L^\dagger [6]. Thus, on the one hand, we may expect large rates for LFV processes due to large $\mu - \tau$ mixing in U_L^\dagger , which at the same time causes large $\nu_\mu - \nu_\tau$ mixing in V^{MNS} for neutrino oscillations, and, on the other hand, difference between V_D and V^{MNS} may be found by neutrino oscillations and LFV processes. If so, important information about GUT structure may be derived then.

The soft breaking terms for the lepton sector is [19],

$$\mathcal{L}_{soft} = -m_{H_1}^2 H_1^\dagger H_1 - m_{H_2}^2 H_2^\dagger H_2 - (m_L^2)^{ij} \tilde{L}_i^\dagger \tilde{L}_j - (m_R^2)^{ij} \tilde{R}_i^* \tilde{R}_j - (m_\nu^2)^{ij} \tilde{\nu}_i^* \tilde{\nu}_j$$

$$\begin{aligned}
& + \left(B\mu H_1 H_2 + \frac{1}{2} B M^{ij} \tilde{\nu}_i^* \tilde{\nu}_j^* + (A_E f_e)^{ij} H_1 \tilde{L}_i \tilde{R}_j \right. \\
& \left. + (A_\nu f_\nu)^{ij} H_2 \tilde{L}_i \tilde{\nu}_j + h.c. \right)
\end{aligned} \tag{2.5}$$

where i, j are generations indices. At M_{GUT} we assume the universal conditions,

$$m_{H_1}^2 = m_{\tilde{H}_1}^2 = m_0^2 \tag{2.6}$$

$$m_L^2 = m_R^2 = m_\nu^2 = m_0^2 \tag{2.7}$$

$$A_E = A_\nu = A_0 \tag{2.8}$$

Fig. 1 gives the explanation of the occurrence of low energy LFV processes. The non-diagonal Yukawa couplings induce $\tilde{\nu}_\mu - \tilde{\nu}_\tau$ mixing through loop effects. This high energy process can be running down by integrating the RGEs to low energy. Thus the study of LFV processes induced by non-universal soft terms can actually reveal high energy fermion flavor structure. In the basis where the f_l is diagonal we can get the non-diagonal scalar mass in the first order of approximation as

$$\begin{aligned}
(\delta \tilde{m}^2)_{23} & \approx \frac{1}{8\pi^2} f_\nu f_\nu^\dagger (3 + a^2) m_0^2 \log \frac{M_{GUT}}{M_R} \\
& \approx \frac{1}{8\pi^2} (V_D)_{23} (V_D)_{33} \cdot f_{\nu_3}^2 (3 + a^2) m_0^2 \log \frac{M_{GUT}}{M_R}
\end{aligned} \tag{2.9}$$

where in the diagonalized Yukawa matrix f_ν^δ only the (3,3) element f_{ν_3} is kept. a is the universal parameter $A_0 = am_0$ and M_R is the scale where the RH neutrinos are decoupled.

B. RGEs running

The RGEs used by us are given in the Appendix A. We have paid much effort to keep the RGEs for the soft terms of lepton sector, which is relevant to our calculations, as complete

as possible. Specially speaking, both the diagonal and non-diagonal terms are kept in the RGEs. However, only diagonal terms of the scalar quark soft terms are kept because these non-diagonal terms are small and not relevant to our calculations. For the Yukawa sector, only the (3,3) elements of the diagonalized Yukawa matrices f_t , f_b , f_τ and f_{ν_3} are kept. The evolution of the mixing matrix V_D from M_{GUT} to M_R is ignored.

The integration procedure consists of iterative runnings of the RGEs from the GUT scale to the low energy scale M_Z and back for every set of inputs of m_0 , $m_{\frac{1}{2}}$, A_0 , $\tan \beta$ and the sign of μ , which are the universal scalar masses, gaugino masses, scalar trilinear parameter, and the standard vacuum expectation values ratio of the two Higgs fields and the Higgsino mass parameter, until the low energy gauge couplings and the Yukawa couplings are all correct within a given range. The parameters μ and B are given by low energy spontaneous breaking conditions [19,20].

The RGEs at Appendix A is given in the basis where f_ν is diagonal. The RH neutrinos are decoupled at M_R . Below M_R the basis is rotated to the basis where f_l is diagonal. The MSSM RGEs are obtained by simply dropping the terms including f_ν and setting V_D equal to 1. The basis rotation leads to

$$\begin{aligned}(m_L^2)_{below} &= V_D(m_L^2)_{up}V_D^\dagger \\ (A_E)_{below} &= V_D(A_E)V_D^\dagger .\end{aligned}\tag{2.10}$$

Below $M_{SUSY} = 250\text{GeV}$ the SM beta functions are used [21]. Threshold effects are taking into account by decoupling the corresponding particles at its running mass $Q = m(Q)$.

Taking $\tan \beta = 2 \sim 10$, we show the numerical results as follows

$$\delta m_L^2 = \begin{pmatrix} 0 & (0.92 \sim 2.87) \times 10^{-3} & (-0.77 \sim -2.06) \times 10^{-3} \\ (0.92 \sim 2.87) \times 10^{-3} & 0 & (0.97 \sim 3.0) \times 10^{-2} \\ (-0.77 \sim -2.06) \times 10^{-3} & (0.97 \sim 3.0) \times 10^{-2} & 0 \end{pmatrix} (3 + a^2)m_0^2 \tag{2.11}$$

$$A_E = \begin{pmatrix} 0.7 & (2.42 \sim 8.12) \times 10^{-4} & (-2.41 \sim -5.88) \times 10^{-4} \\ (2.42 \sim 8.12) \times 10^{-4} & 0.7 & (2.5 \sim 8.67) \times 10^{-3} \\ (-2.41 \sim -5.88) \times 10^{-4} & (2.5 \sim 8.67) \times 10^{-3} & 0.7 \end{pmatrix} A_0 \quad (2.12)$$

where smaller $\tan \beta$ may give larger contribution.

C. Low energy supersymmetric spectrum

At low energy the supersymmetric particle masses and mixing angles are obtained by diagonalizing the corresponding chargino, neutralino, scalar neutrino and scalar lepton mass matrices numerically. The slepton mass matrix is given by a 6×6 matrix as

$$m_l^2 = \begin{pmatrix} m_{LL} & m_{LR} \\ m_{LR}^\dagger & m_{RR} \end{pmatrix} \quad (2.13)$$

where m_{LL} , m_{LR} , m_{RR} are all 3×3 matrices given by

$$\begin{aligned} (m_{LL})_{ij} &= (m_L^2)_{ij} + (m_l^2)\delta_{ij} + M_Z^2(-\frac{1}{2} + \sin^2 \theta_W) \cos 2\beta \delta_{ij} , \\ (m_{LR})_{ij} &= -((A_E)^{ij} + \mu \tan \beta \delta^{ij}) m_l^j , \\ (m_{RR})_{ij} &= (m_R^2 + m_l^2 - M_Z^2 \sin^2 \theta_W \cos 2\beta) \delta_{ij} . \end{aligned} \quad (2.14)$$

The m_R^2 is diagonal since only f_l enters its RGE. The full sneutrino mass matrix has a 12×12 structure. However, according to [10,11] if we only keep the first order of these terms perturbed by RH neutrino masses we can have a very simple structure, which is relevant to generation mixing,

$$m_\nu^2 = m_L^2 + \frac{1}{2} M_Z^2 \cos 2\beta . \quad (2.15)$$

The mass matrices of chargino and neutrino are standard and given at Appendix B.

III. ANALYTIC FORMULAS

Fig. 2 gives the one loop diagrams relevant to the process $\tau \rightarrow \mu\gamma$. The amplitude of this process can be written in the general form

$$M = em_i \bar{u}_j(p_2) i\sigma_{\mu\nu} p_3^\nu (A_L P_L + A_R P_R) u_i(p_1) \epsilon^\mu(p_3) , \quad (3.1)$$

where $P_{L,R} = \frac{1}{2}(1 \mp \gamma_5)$ are the chirality projection operators. i, j represent initial and final lepton flavor. The most convenient way to calculate A_L and A_R is to pick up the one loop momentum integral contributions which are proportional to $\bar{u}_j(p_2) P_{L,R} u_i(p_1) 2p_1 \cdot \epsilon$ respectively. The neutralino exchanging contribution is

$$A_L^{(n)} = \frac{1}{32\pi^2} \left(\frac{e}{\sqrt{2} \cos \theta} \right)^2 \frac{1}{m_{\tilde{l}_\alpha}^2} \left[B^{j\alpha a*} B^{i\alpha a} \frac{1 - 6k + 3k^2 + 2k^3 - 6k^2 \log k}{6(1-k)^4} + \frac{m_{\chi_a^0}}{m_i} B^{j\alpha a*} A^{i\alpha a} \frac{1 - k^2 + 2k \log k}{(1-k)^3} \right] , \quad (3.2)$$

$$A_R^{(n)} = A_L^{(n)} (B \leftrightarrow A) , \quad (3.3)$$

where $k = m_{\chi_a^0}^2 / m_{\tilde{l}_\alpha}^2$. A and B are the lepton-slepton-neutralino coupling vertices given in Appendix B. The corresponding contribution coming from exchanging charginos are

$$A_L^{(c)} = -\frac{g_2^2}{32\pi^2} Z_\nu^{i\alpha*} Z_\nu^{j\alpha} \frac{1}{m_{\tilde{\nu}_\alpha}^2} \left[Z_{2a}^- Z_{2a}^{-*} \frac{m_i m_j}{2M_W^2 \cos^2 \beta} \frac{2 + 3k - 6k^2 + k^3 + 6k \log k}{6(1-k)^4} + \frac{m_{\chi_a^-}}{\sqrt{2}M_W \cos \beta} Z_{1a}^+ Z_{2a}^- \frac{m_j}{m_i} \frac{3 - 4k + k^2 + 2 \log k}{(1-k)^3} \right] , \quad (3.4)$$

$$A_R^{(c)} = -\frac{g_2^2}{32\pi^2} Z_\nu^{i\alpha*} Z_\nu^{j\alpha} \frac{1}{m_{\tilde{\nu}_\alpha}^2} \left[Z_{1a}^+ Z_{1a}^{+*} \frac{2 + 3k - 6k^2 + k^3 + 6k \log k}{6(1-k)^4} + \frac{m_{\chi_a^-}}{\sqrt{2}M_W \cos \beta} Z_{1a}^+ Z_{2a}^- \frac{3 - 4k + k^2 + 2 \log k}{(1-k)^3} \right] , \quad (3.5)$$

where $k = m_{\chi_a^-}^2 / m_{\tilde{\nu}_\alpha}^2$. Mixing matrices Z_ν , Z^+ and Z^- are given in Appendix B.

The branching ratio is given by

$$BR(\tau \rightarrow \mu\gamma) = \frac{\alpha_{em}}{4\pi} m_i^5 (|A_L|^2 + |A_R|^2) / \Gamma_\tau \quad , \quad (3.6)$$

where $\Gamma_\tau = 2.265 \times 10^{-12} GeV$.

Fig. 3 gives the diagrams contributing to the $Z \rightarrow \tau\mu$ process. Neglecting masses of the final fermions the amplitude is given as $M = \sum_i a_i M_i$, where M_i are

$$M_{1,2} = \bar{u}(p_2) \gamma^\mu P_{L,R} v(p_1) \epsilon_\mu \quad , \quad (3.7)$$

$$M_{3,4} = \bar{u}(p_2) P_{L,R} v(p_1) p_1 \cdot \epsilon \quad (3.8)$$

respectively. The corresponding analytic expressions of a_i are given in appendix C.

The branching ratio for $Z \rightarrow \tau\mu$ is given by $Br(Z \rightarrow \mu\tau) = \Gamma(Z \rightarrow \tau^\pm \mu^\mp) / \Gamma_Z$, where $\Gamma_Z = 2.49 GeV$ and

$$\begin{aligned} \Gamma(Z \rightarrow \mu\tau) &= \frac{1}{48\pi M_Z} \cdot \sum |M|^2 \\ &= \frac{1}{48\pi M_Z} \cdot \left[(|a_1|^2 + |a_2|^2) \cdot 2M_Z^2 + (|a_3|^2 + |a_4|^2) \cdot \frac{M_Z^4}{4} \right] \quad , \end{aligned} \quad (3.9)$$

where Σ represents the sum of μ, τ spins and Z polarizations.

IV. A SO(10) GRAND UNIFIED MODEL

To give definite predictions we will work within a specific model. Before we turn to introduce this model it is worth noting that our calculations are not very model sensitive. That is the reason why we concentrate on the 2–3 generation mixing. The mixing between the first two generations may be very sensitive to different models and we will discuss the processes separately. From Fig.1, we know that $\tau - \mu$ mixing is mainly determined by the factor $\delta \tilde{m}_{23}^2 / m_0^2$, which, from Eq. (2.9), depends only on the parameters $(V_D)_{23} \cdot (V_D)_{33}$,

f_{ν_3} , M_{GUT} and M_R . $M_{GUT} \approx 2 \times 10^{16} GeV$ is required by any supersymmetric grand unified model. In the context of $SO(10)$ grand unified models f_{ν_3} is related to the top Yukawa coupling f_t at the GUT scale. In addition, with the SuperK data of $m_{\nu_\tau} \approx \frac{1}{20} eV$ $M_R \approx 2 \times 10^{14} GeV$ is roughly determined by the see-saw mechanism. Thus the only model sensitive parameter in fermion textures is $(V_D)_{23}$ ($(V_D)_{33}$ is determined by unitary condition of the V_D matrix). In most published $SO(10)$ models the large $\nu_\mu - \nu_\tau$ mixing is not produced dominantly by M_R mass matrix and thus produce large $\mu - \tau$ mixing, for example, we have $(V_D)_{23} \cdot (V_D)_{33} \sim (0.5 - 0.3)$ corresponding to $\theta_{23} \sim (20^\circ - 70^\circ)$. Thus our discussions on these branching ratios are useful for estimating the predictions for such a class of unified models, although they may be different in details.

We did our calculations within the model given by Albright *et al* [15]. The model gives excellent predictions of quark and lepton masses and naturally explains the largeness of $\nu_\mu - \nu_\tau$ mixing and the smallness of V_{cb} . At M_{GUT} , after the $SO(10)$ breaking to the MSSM, the fermion mass textures are given by

$$U = \begin{pmatrix} \eta & 0 & 0 \\ 0 & 0 & -\epsilon/3 \\ 0 & \epsilon/3 & 1 \end{pmatrix} M_U, \quad D = \begin{pmatrix} 0 & \delta & \delta' e^{i\phi} \\ \delta & 0 & -\epsilon/3 \\ \delta' e^{i\phi} & \sigma + \epsilon/3 & 1 \end{pmatrix} M_D, \quad (4.1)$$

$$N = \begin{pmatrix} \eta & 0 & 0 \\ 0 & 0 & \epsilon \\ 0 & -\epsilon & 1 \end{pmatrix} M_U, \quad L = \begin{pmatrix} 0 & \delta & \delta' e^{i\phi} \\ \delta & 0 & \sigma + \epsilon \\ \delta' e^{i\phi} & -\epsilon & 1 \end{pmatrix} M_D, \quad (4.2)$$

where U , D , N and L are the up quark, down quark, neutrino and lepton mass matrices respectively. The most remarkable feature of the textures is the lopsided parameter $\sigma \sim 1$ at L and D . According to the $SU(5)$ relation $D = L^T$, the large $\nu_\mu - \nu_\tau$ mixing due to the σ term in L is related to the right-handed down quark mixing, which has no observable physical effects. The smallness of quark mixing V_{cb} is determined by the parameter $\epsilon \sim 0.1$,

which translates to the right-handed lepton mixing.

The model predicts the lepton sector 2-3 mixing with $\theta_{23} \sim 63^\circ$, which leads to the only model structure sensitive quantity for our processes $(V_D)_{23} \cdot (V_D)_{33} \sim 0.4$.

Taking all the fermion masses and V_{KM} elements at M_Z given in Ref. [22] as inputs, we calculate the corresponding values at M_{GUT} with several values of $\tan\beta$ by integrating the RGEs and fit the parameters in Eq. (4.1) and (4.2). We find these parameters are not sensitive to the supersymmetric parameters, except that M_U becomes larger as taking small $\tan\beta$. To keep the predicted neutrino masses in the correct range we take $M_R = 5 \times 10^{14} GeV$ when $\tan\beta = 2$ and $M_R = 2 \times 10^{14} GeV$ when $\tan\beta = 5, 10$ in our later calculations.

V. NUMERICAL RESULT AND DISCUSSION

The relevant parameters on predicting the branching ratios are the universal supersymmetry soft breaking parameters, $m_0, m_{\frac{1}{2}}, A_0, \tan\beta$ and the lepton sector mixing matrix V_D defined in Eq. (2.3). We will present dependence of the branching ratio of the processes $\tau \rightarrow \mu\gamma$ and $Z \rightarrow \tau\mu$ on the soft parameters in the model of [15]. In our calculations the soft parameters are constrained by various theoretical and experimental considerations [23], such as the LSP of the model should be a neutralino and masses of all supersymmetric particles be beyond present mass limits and so on.

In Figs. 4~7, we plot the branching ratio of $\tau \rightarrow \mu\gamma$ as functions of m_0 for several sets of other soft parameters. Two experimental bounds are plotted in every figure, which correspond to the present experimental limit $BR(\tau \rightarrow \mu\gamma) < 1.1 \times 10^{-6}$ [24] and the expected sensitivity of future experiments $BR(\tau \rightarrow \mu\gamma) < 1.0 \times 10^{-9}$ [10]. The general trend of $BR(\tau \rightarrow \mu\gamma)$ is decreasing dramatically as m_0 increases. In Fig. 4, the branching ratio is plotted for $m_{\frac{1}{2}} = 100 GeV$, $\tan\beta = 5$ and $A_0 = 2m_0, m_0, 0$, taking μ either positive

or negative. That branching ratio decreases with $a = A_0/m_0$ is easily understood due to the Eq. (1). It is interesting to note that although this process can not be observed at present, it will be detectable in the future experiments in a large part of the soft parameter space.

Fig. 5 presents the branching ratio for $m_{\frac{1}{2}} = 100, 200, 400 GeV$ and $A_0 = m_0, \tan \beta = 5$. We can find that the branching ratio is also very sensitive to the parameter $m_{\frac{1}{2}}$. It will decrease quickly with increasing $m_{\frac{1}{2}}$. If $m_{\frac{1}{2}} > 400 GeV$, this process will be non-observable as displayed in the figure. In Fig. 6, we plot the branching ratio for $m_{\frac{1}{2}} = 100 GeV$, $\tan \beta = 10$ and $A_0 = \pm 2m_0, \pm m_0, 0$. We find that the sign of A_0 is not very important in the order of magnitude estimate. However, the sign of A_0 is still relevant to the precise predictions. Fig. 7 plots the branching ratio at different $\tan \beta$. The branching ratio increases as $\tan \beta$ becomes large. It is explained in Ref. [12] that the dominant term of the amplitude for $\tau \rightarrow \mu \gamma$ is proportional to $\tan \beta$. We note that at $\tan \beta = 2$ the sign of μ can be significant. The branching ratio when μ is negative is much smaller than that when μ is positive.

In Figs. 8~10, we present the quantitative results of the branching ratio of the decay $Z \rightarrow \tau \mu$. We find in most parameter space this process can not be detected by the Giga-Z option [17]. However, we can still find several interesting features in this process which are different from the τ radiative decay process. The most remarkable feature about this LFV process is that its branching ratio becomes large at first and then approaches to a constant when m_0 is increasing, which gives a sharp contrast with the process $\tau \rightarrow \mu \gamma$. Thus this process may have advantage over the $\tau \rightarrow \mu \gamma$ process in some region of parameter space. The reason for this different behavior between the two processes can be traced back to the different coupling structures between the processes as shown in Eqs. (3.1) and (3.7), (3.8). The magnetic structure of τ decay determines that its amplitude is inversely proportional to the sfermion masses square, whereas there is a vector current coupling in Eq. (3.7) which

determines the $Z \rightarrow \mu\tau$ amplitude's trend as increasing m_0 .

Fig. 8 shows the branching ratio as a function of m_0 for $m_{\frac{1}{2}} = 100\text{GeV}$, $\tan\beta = 5$ and $A_0 = 2m_0$, $m_0, 0$ with both positive and negative sign of μ . The sign of μ is quite irrelevant when $m_0 > 500\text{GeV}$. Fig. 9 displays the same function for different $m_{\frac{1}{2}}$ values, 100, 200, 400GeV, with $A_0 = 2m_0$ and $\tan\beta = 5$. The dependence of $BR(Z \rightarrow \tau\mu)$ on a and $m_{\frac{1}{2}}$ is similar to that of $BR(\tau \rightarrow \mu\gamma)$. We note again that the sign of μ is irrelevant when $m_{\frac{1}{2}} > 200\text{GeV}$. Fig. 10 gives the branching ratio for $\tan\beta = 2, 5, 10$ with $A_0 = 2.5m_0$, $m_{\frac{1}{2}} = 150\text{GeV}$. We can see another important feature of this LFV process that it is more favorable for the small $\tan\beta$ value in contrast with the $\tau \rightarrow \mu\gamma$ process. At the extreme case, the branching ratio may access 1×10^{-8} , which may be detectable. The relationship between the branching ratio and $\tan\beta$ is easily understood. For small $\tan\beta$ large non-universal soft mass term $\delta\tilde{m}_{23}^2$ will be produced due to a large f_{ν_3} in Eq. (2.9). We note that when $\tan\beta$ becomes smaller, the $BR(Z \rightarrow \tau\mu)$ increases quickly.

In summary, according to our calculations we find that the $\tau \rightarrow \mu\gamma$ is more feasible than $Z \rightarrow \tau\mu$ to reveal charged lepton flavor violation in the context of SO(10) SUSY-GUTs. In most parameter space $\tau \rightarrow \mu\gamma$ has a branching ratio that can be detected in the future experiments [10]. The $Z \rightarrow \tau\mu$ is hopeful to be detected in a small parameter space. We note the remarkable feature of the Z decay process that its dependence on the supersymmetry soft parameters $\tan\beta$ and m_0 is opposite to that of τ decay. Thus it can supplement the LFV search besides the $\tau \rightarrow \mu\gamma$ process.

VI. SUMMARY AND CONCLUSION

In this work, we present the dependence of the branching ratios of two charged lepton flavor violation processes $\tau \rightarrow \mu\gamma$ and $Z \rightarrow \tau\mu$ on the supersymmetry soft breaking parameters

in the context of SO(10) grand unified models with the "lopsided" texture of mass matrices for charged leptons and down quarks. We expect these processes may be detected in the future experiments. The first process is more hopeful to be observed. The second process may offer useful information about the soft parameters if it is also observed. The different behaviors of the two processes depending on $\tan\beta$ and m_0 implies that the simultaneous study of the two processes will be interesting.

We expect the study of charged lepton flavor process may provide another window of high energy physics besides the neutrino oscillation study. The combined study of the LFV processes and neutrino oscillation may feed light on the sector of right-handed neutrinos, which may be necessary in a model to naturally explain the small neutrino masses.

ACKNOWLEDGMENTS

Y-B. Dai's work is supported by the National Science Foundation of China.

Appendix A

In this appendix we give the renormalization group equations of the MSSM supplemented with RH neutrinos [12,13]. The two-loop RGEs of the gauge couplings can be found in many literatures which will not be affected by the presence of the RH neutrinos. We give one-loop RGEs of the Yukawa coupling matrices and the soft terms which are affected by the presence of RH neutrinos. In this appendix we denote the Yukawa couplings of up quark, down quark, lepton and neutrino as U , D , E and N respectively. Denote the soft terms as $A_U \cdot U = U_A$ and so on. The RGEs of the Yukawa couplings are

$$\frac{dU}{dt} = \frac{1}{16\pi^2} \left[-\Sigma c_i g_i^2 + 3UU^\dagger + DD^\dagger + Tr[3UU^\dagger + NN^\dagger] \right] U \quad , \quad (\text{A.1})$$

$$\frac{dD}{dt} = \frac{1}{16\pi^2} \left[-\Sigma c_i' g_i^2 + 3DD^\dagger + UU^\dagger + Tr[3DD^\dagger + EE^\dagger] \right] D \quad , \quad (A.2)$$

$$\frac{dE}{dt} = \frac{1}{16\pi^2} \left[-\Sigma c_i'' g_i^2 + 3EE^\dagger + NN^\dagger + Tr[3DD^\dagger + EE^\dagger] \right] E \quad , \quad (A.3)$$

$$\frac{dN}{dt} = \frac{1}{16\pi^2} \left[-\Sigma c_i''' g_i^2 + 3NN^\dagger + EE^\dagger + Tr[3UU^\dagger + NN^\dagger] \right] N \quad , \quad (A.4)$$

where $t = \log Q$, $c_i = (\frac{13}{15}, 3, \frac{16}{3})$, $c_i' = (\frac{7}{15}, 3, \frac{16}{3})$, $c_i'' = (\frac{9}{5}, 3, 0)$, $c_i''' = (\frac{3}{5}, 3, 0)$. The RGEs of μ and soft parameters of Higgs sector are

$$\frac{d\mu}{dt} = \frac{1}{16\pi^2} \left[-\Sigma c_i''' g_i^2 + Tr[3UU^\dagger + 3DD^\dagger + EE^\dagger + NN^\dagger] \right] \mu \quad , \quad (A.5)$$

$$\frac{dB}{dt} = \frac{2}{16\pi^2} \left[-\Sigma c_i''' g_i^2 M_i + Tr[3UU_A + 3DD_A + EE_A + NN_A] \right] \quad , \quad (A.6)$$

$$\begin{aligned} \frac{dm_{H_U}^2}{dt} = & \frac{2}{16\pi^2} \left[-\Sigma c_i''' g_i^2 M_i^2 + 3Tr[U(M_{Q_L}^2 + M_{U_R}^2)U^\dagger + m_{H_U}^2 UU^\dagger + U_A U_A^\dagger] \right. \\ & \left. + Tr[M_{Q_L}^2 NN^\dagger + NM_{\bar{\nu}_R}^2 N^\dagger + m_{H_U}^2 NN^\dagger + N_A N_A^\dagger] \right] \quad , \end{aligned} \quad (A.7)$$

$$\begin{aligned} \frac{dm_{H_D}^2}{dt} = & \frac{2}{16\pi^2} \left[-\Sigma c_i''' g_i^2 M_i^2 + 3Tr[D(M_{Q_L}^2 + M_{D_R}^2)D^\dagger + m_{H_D}^2 DD^\dagger + D_A D_A^\dagger] \right. \\ & \left. + Tr[E(M_L^2 + M_R^2)E^\dagger + m_{H_D}^2 EE^\dagger + E_A E_A^\dagger] \right] \quad . \end{aligned} \quad (A.8)$$

M_i in the above expressions are the gaugino masses whose RGEs are same as those in the MSSM.

Then we give RGEs of soft mass terms of lepton sector

$$\begin{aligned} \frac{dM_L^2}{dt} = & \frac{2}{16\pi^2} \left[-\Sigma c_i''' g_i^2 M_i^2 + \frac{1}{2}[NN^\dagger M_L^2 + M_L^2 NN^\dagger] + \frac{1}{2}[EE^\dagger M_L^2 + M_L^2 EE^\dagger] \right. \\ & \left. + EM_R^2 E^\dagger + m_{H_D}^2 EE^\dagger + E_A E_A^\dagger + NM_{\bar{\nu}_R}^2 N^\dagger + m_{H_U}^2 NN^\dagger + N_A N_A^\dagger \right] \quad , \end{aligned} \quad (A.9)$$

$$\frac{dM_R^2}{dt} = \frac{2}{16\pi^2} \left[-\frac{12}{5} g_1^2 M_1^2 + E^\dagger EM_R^2 + M_R^2 E^\dagger E + 2(E^\dagger M_L^2 E + m_{H_D}^2 E^\dagger E + E_A^\dagger E_A) \right] \quad , \quad (A.10)$$

$$\frac{dM_{\bar{\nu}_R}^2}{dt} = \frac{2}{16\pi^2} \left[N^\dagger NM_{\bar{\nu}_R}^2 + M_{\bar{\nu}_R}^2 N^\dagger N + 2(N^\dagger M_L^2 N + m_{H_U}^2 N^\dagger N + N_A^\dagger N_A) \right] \quad . \quad (A.11)$$

The RGEs of trilinear terms of lepton sector are

$$\frac{dA_E}{dt} = \frac{1}{16\pi^2} \left[-2\Sigma c_i'' g_i^2 M_i + 2Tr(3A_D DD^\dagger + A_E EE^\dagger) + 2A_N NN^\dagger \right]$$

$$+(5EE^\dagger + NN^\dagger)A_E + A_E(EE^\dagger - NN^\dagger) \Big] , \quad (\text{A.12})$$

$$\begin{aligned} \frac{dA_N}{dt} = & \frac{1}{16\pi^2} \left[-2\Sigma c_i''' g_i^2 M_i + 2\text{Tr}(3A_U U U^\dagger + A_N N N^\dagger) + 2A_E E E^\dagger \right. \\ & \left. + (5NN^\dagger + EE^\dagger)A_N + A_N(N^\dagger - EE^\dagger) \right] . \end{aligned} \quad (\text{A.13})$$

In the basis where N is diagonal and only keep the third family Yukawa coupling constants

f_t, f_b, f_{ν_3} and f_τ , then the RGEs are simplified as

$$\frac{df_t}{dt} = \frac{1}{16\pi^2} \left[-\Sigma c_i g_i^2 + 6f_t^2 + f_b^2 + f_{\nu_3}^2 \right] f_t , \quad (\text{A.14})$$

$$\frac{df_b}{dt} = \frac{1}{16\pi^2} \left[-\Sigma c_i' g_i^2 + 6f_b^2 + f_t^2 + f_\tau^2 \right] f_b , \quad (\text{A.15})$$

$$\frac{df_{\nu_3}}{dt} = \frac{1}{16\pi^2} \left[-\Sigma c_i''' g_i^2 + 4f_{\nu_3}^2 + 3f_t^2 + f_\tau^2 |V_{33}|^2 \right] f_{\nu_3} , \quad (\text{A.16})$$

$$\frac{df_\tau}{dt} = \frac{1}{16\pi^2} \left[-\Sigma c_i'' g_i^2 + 4f_\tau^2 + 3f_b^2 + f_{\nu_3}^2 |V_{33}|^2 \right] f_\tau , \quad (\text{A.17})$$

$$\frac{d\mu}{dt} = \frac{1}{16\pi^2} \left[-\Sigma c_i''' g_i^2 + 3f_t^2 + 3f_b^2 + f_{\nu_3}^2 + f_\tau^2 \right] \mu \quad (\text{A.18})$$

$$\frac{dB}{dt} = \frac{2}{16\pi^2} \left[-\Sigma c_i''' g_i^2 M_i + 3f_t^2 A_t + 3f_b^2 A_b + f_{\nu_3}^2 A_{\nu_3} + f_\tau^2 A_\tau \right] \quad (\text{A.19})$$

$$\begin{aligned} \frac{dm_{H_U}^2}{dt} = & \frac{2}{16\pi^2} \left[-\Sigma c_i''' g_i^2 M_i^2 + 3f_t^2 (M_{\tilde{t}_L}^2 + M_{\tilde{t}_R}^2 + m_{H_U}^2 + A_t^2) \right. \\ & \left. + f_{\nu_3}^2 (M_{\tilde{\tau}_L}^2 + M_{\tilde{\tau}_R}^2 + m_{H_U}^2 + A_{\nu_3}^2) \right] , \end{aligned} \quad (\text{A.20})$$

$$\begin{aligned} \frac{dm_{H_D}^2}{dt} = & \frac{2}{16\pi^2} \left[-\Sigma c_i''' g_i^2 M_i^2 + 3f_b^2 (M_{\tilde{t}_L}^2 + M_{\tilde{b}_R}^2 + m_{H_D}^2 + A_b^2) \right. \\ & \left. + f_\tau^2 (M_{\tilde{\tau}_L}^2 + M_{\tilde{\tau}_R}^2 + m_{H_D}^2 + A_\tau^2) \right] , \end{aligned} \quad (\text{A.21})$$

$$\begin{aligned} \left(\frac{M_{\tilde{L}}^2}{dt} \right)_{ij} = & \frac{2}{16\pi^2} \left[(-\Sigma c_i''' g_i^2 M_i^2) \delta_{ij} + V_{3i}^* V_{3j} f_\tau^2 \left(\frac{1}{2} ((M_{\tilde{L}}^2)_{ii} + (M_{\tilde{L}}^2)_{jj}) + M_{\tilde{\tau}_R}^2 + m_{H_D}^2 + (A_E)_{ii} (A_E)_{jj} \right) \right. \\ & \left. + f_{\nu_3}^2 \left(\frac{1}{2} ((M_{\tilde{L}}^2)_{3j} \delta_{3i} + (M_{\tilde{L}}^2)_{i3} \delta_{3j}) + m_{\tilde{\nu}_3}^2 \delta_{i3} \delta_{j3} + M_{H_U}^2 \delta_{i3} \delta_{j3} + (A_\nu)_{i3} (A_\nu)_{j3} \right) \right] , \end{aligned} \quad (\text{A.22})$$

$$\left(\frac{dm_{\tilde{R}}}{dt} \right)_{ii} = \frac{2}{16\pi^2} \left[-\frac{12}{5} g_1^2 M_1^2 + 2f_\tau^2 ((M_{\tilde{L}}^2)_{ii} + (M_{\tilde{R}}^2)_{ii} + m_{H_D}^2 + A_\tau^2) \delta_{i3} \right] , \quad (\text{A.23})$$

$$\left(\frac{dm_{\tilde{\nu}_R}}{dt} \right)_{ii} = \frac{2}{16\pi^2} \left[2f_{\nu_3}^2 ((M_{\tilde{L}}^2)_{ii} + (M_{\tilde{\nu}_R}^2)_{ii} + m_{H_U}^2 + A_{\nu_3}^2) \right] \delta_{i3} , \quad (\text{A.24})$$

$$\frac{dA_t}{dt} = \frac{2}{16\pi^2} \left[-\Sigma c_i g_i^2 M_i + 6f_t^2 A_t + f_b^2 A_b + f_{\nu_3}^2 A_{\nu_3} \right] , \quad (\text{A.25})$$

$$\frac{dA_b}{dt} = \frac{2}{16\pi^2} \left[-\Sigma c_i' g_i^2 M_i + 6f_b^2 A_b + f_\tau^2 A_\tau + f_t^2 A_t \right] , \quad (\text{A.26})$$

$$\left(\frac{dA_E}{dt}\right)_{ij} = \frac{1}{16\pi^2} \left[(-2\Sigma c_i'' g_i^2 M_i + 6f_b^2 A_b + 2f_\tau^2 A_\tau) \delta_{ij} + V_{3i}^* V_{3j} f_\tau^2 (5(A_E)_{jj} + (A_E)_{ii}) + f_{\nu_3}^2 (2(A_\nu)_{i3} \delta_{j3} + (A_E)_{3j} \delta_{i3} - (A_E)_{i3} \delta_{j3}) \right] , \quad (\text{A.27})$$

$$\left(\frac{dA_\nu}{dt}\right)_{ij} = \frac{1}{16\pi^2} \left[(-2\Sigma c_i''' g_i^2 M_i + 6f_t^2 A_t + 2f_{\nu_3}^2 A_{\nu_3}) \delta_{ij} + V_{3i}^* V_{3j} f_\tau^2 (2(A_E)_{ii} + (A_\nu)_{ii} - (A_\nu)_{ii}) + f_{\nu_3}^2 (5(A_\nu)_{3j} \delta_{i3} + (A_\nu)_{i3} \delta_{j3}) \right] . \quad (\text{A.28})$$

The matrix V in the above equations refers to V_D defined in Eq. (2.3). Below M_R , RH neutrinos are decoupled and the RGEs of the MSSM are used. This can be achieved by setting $f_{\nu_3} = 0$ and $V_{ij} = \delta_{ij}$ in the above expressions.

Appendix B

In this appendix we list the relevant pieces of the Lagrangian and conventions which we take in our calculations [19]. The Lagrangian pieces are

$$\mathcal{L}_{\tilde{\nu}\tilde{\nu}Z} = \frac{-ig_2}{2\cos\theta_W} (\tilde{\nu}^{I*} \overleftrightarrow{\partial}_\mu \tilde{\nu}^J) Z^\mu , \quad (\text{B.1})$$

$$\mathcal{L}_{\tilde{l}\tilde{l}Z} = \frac{ig_2}{\cos\theta_W} \left(\frac{1}{2} Z_L^{Ii} Z_L^{Ij*} - \sin^2\theta_W \delta_{ij} \right) (\tilde{l}_i^* \overleftrightarrow{\partial}_\mu \tilde{l}_j) Z^\mu , \quad (\text{B.2})$$

$$\mathcal{L}_{\chi^+\chi^-Z} = \frac{g_2}{2\cos\theta_W} \chi_j^- \gamma^\mu [Z_{1j}^{+*} Z_{1i}^+ P_R + Z_{1j}^- Z_{1i}^{*-} P_L + \delta_{ij} \cos 2\theta_W] \chi_i^- Z_\mu , \quad (\text{B.3})$$

$$\begin{aligned} \mathcal{L}_{\chi^0\chi^0Z} &= \frac{g_2}{2\cos\theta_W} \bar{\chi}_i^0 \gamma^\mu [(Z_N^{4i*} Z_N^{4j} - Z_N^{3i*} Z_N^{3j}) P_L - (Z_N^{4i} Z_N^{4j*} - Z_N^{3i} Z_N^{3j*}) P_R] \chi_j^0 Z_\mu \\ &= \frac{g_2}{2\cos\theta_W} \bar{\chi}_i^0 \gamma^\mu [C^{ij} P_L + D^{ij} P_R] \chi_j^0 Z_\mu , \end{aligned} \quad (\text{B.4})$$

$$\mathcal{L}_{\chi^+l\tilde{\nu}} = -g_2 \bar{l}^I \left[Z_{1i}^{+*} P_R - \frac{m_{lI}}{\sqrt{2}M_W \cos\beta} Z_{2i}^- P_L \right] Z_\nu^{IJ} \chi_i^- \tilde{\nu}_J + h.c. \quad (\text{B.5})$$

$$\begin{aligned} \mathcal{L}_{\chi^0l\tilde{l}} &= \frac{e}{\sqrt{2}\cos\theta_W} \bar{\chi}_j^0 \left[\left(Z_L^{Ii} (Z_N^{1j} + Z_N^{2j} \cot\theta_W) - \cot\theta_W \frac{m_{lI}}{M_W \cos\beta} Z_L^{(I+3)i} Z_N^{3j} \right) P_L \right. \\ &\quad \left. - \left(2Z_L^{(I+3)i} Z_N^{1j*} + \cot\theta_W \frac{m_{lI}}{M_W \cos\beta} Z_L^{Ii} Z_N^{3j*} \right) P_R \right] l^I \tilde{l}_i^* + h.c. \\ &= \frac{e}{\sqrt{2}\cos\theta_W} \bar{\chi}_j^0 [A^{Iij} P_L + B^{Iij} P_R] l^I \tilde{l}_i^* + h.c. \end{aligned} \quad (\text{B.6})$$

The abbreviations defined in the above expressions will be used in the next Appendix.

The mixing matrices Z in the above expressions are given below. The scalar lepton and scalar neutrino mass matrices are given in Sec II. The corresponding mixing matrices are defined as

$$Z_L^\dagger m_l^2 Z_L = \text{diag} \left(m_{l_i}^2 \right), \quad i = 1 \dots 6 \quad (\text{B.7})$$

$$Z_\nu^\dagger m_\nu^2 Z_\nu = \text{diag} \left(m_{\nu_i}^2 \right), \quad i = 1, 2, 3 \quad (\text{B.8})$$

The mass matrix of charginos is

$$M_\chi = \begin{bmatrix} m_2 & \sqrt{2} M_W \sin \beta \\ \sqrt{2} M_W \cos \beta & \mu \end{bmatrix}. \quad (\text{B.9})$$

The mixing matrices Z^\pm is defined as

$$(Z^-)^T M_\chi Z^+ = \text{diag} (m_{\chi_1}, m_{\chi_2}) . \quad (\text{B.10})$$

The mass matrix for neutralinos is

$$M_{\chi^0} = \begin{bmatrix} m_1 & 0 & -M_Z \cos \beta \sin \theta_W & M_Z \sin \beta \sin \theta_W \\ 0 & m_2 & M_Z \cos \beta \cos \theta_W & -M_Z \sin \beta \cos \theta_W \\ -M_Z \cos \beta \sin \theta_W & M_Z \cos \beta \cos \theta_W & 0 & -\mu \\ M_Z \sin \beta \sin \theta_W & -M_Z \sin \beta \cos \theta_W & -\mu & 0 \end{bmatrix}, \quad (\text{B.11})$$

which is diagonalized by

$$Z_N^T M_{\chi^0} Z_N = \text{diag} \left(m_{\chi_1^0}, m_{\chi_2^0}, m_{\chi_3^0}, m_{\chi_4^0} \right) . \quad (\text{B.12})$$

Appendix C

In this appendix we give the analytic expressions of a_i defined in Sec III.

a_1 is given by

$$a_1 = \frac{g_2}{2 \cos \theta_W} \frac{g_2^2}{16\pi^2} (a_1(a) + a_1(b) + a_1(c) + a_1(d) + 2a_1(e) + 2a_1(f)) , \quad (\text{C.1})$$

where $a_1(i)$ is coming from the corresponding Feynman diagram. They are given by

$$a_1(a) = |Z_{1a}^+|^2 Z_\nu^{i\alpha} Z_\nu^{j\alpha*} (-2) C_{00} , \quad (\text{C.2})$$

$$a_1(b) = -\tan^2 \theta_W \left(\frac{1}{2} Z_L^{I\alpha} Z_L^{I\beta} - \sin^2 \theta_W \delta^{\alpha\beta} \right) (-2) A^{i\alpha a*} A^{j\beta a} C_{00} , \quad (\text{C.3})$$

$$a_1(c) = -Z_{1a}^{+*} Z_{1b}^+ Z_\nu^{i\alpha} Z_\nu^{j\alpha*} \left[\left((Z_{1b}^- Z_{1a}^{-*} + \delta^{ab} \cos 2\theta_W) m_{\chi_a^-} m_{\chi_b^-} - (Z_{1b}^{+*} Z_{1a}^+ + \delta^{ab} \cos 2\theta_W) m_{\tilde{\nu}_\alpha}^2 \right) C_0 \right. \\ \left. - (Z_{1b}^{+*} Z_{1a}^+ + \delta^{ab} \cos 2\theta_W) (B_0 - 2C_{00}) \right] , \quad (\text{C.4})$$

$$a_1(d) = -\frac{1}{2} \tan^2 \theta_W A^{i\alpha a*} A^{j\alpha b} \left[2D^{ab} C_{00} + \left(C^{ab} m_{\chi_a^0} m_{\chi_b^0} - D^{ab} m_{\tilde{l}_\alpha}^2 \right) C_0 - D^{ab} B_0 \right] , \quad (\text{C.5})$$

$$a_1(e) = -2(0.5 - \sin^2 \theta_W) |Z_{1a}^+|^2 Z_\nu^{i\alpha} Z_\nu^{j\alpha*} (B_0 + B_1) , \quad (\text{C.6})$$

$$a_1(f) = -\tan^2 \theta_W (0.5 - \sin^2 \theta_W) A^{i\alpha a*} A^{j\alpha a} (B_0 + B_1) , \quad (\text{C.7})$$

where i, α and a represent the flavors of lepton, slepton or sneutrino and chargino or neutralino respectively. a_2 is given by

$$a_2 = \frac{g_2}{2 \cos \theta_W} \frac{g_2^2}{16\pi^2} (a_2(b) + a_2(d) + 2a_2(f)) , \quad (\text{C.8})$$

where

$$a_2(b) = -\tan^2 \theta_W \left(\frac{1}{2} Z_L^{I\alpha} Z_L^{I\beta} - \sin^2 \theta_W \delta^{\alpha\beta} \right) (-2) B^{i\alpha a*} B^{j\alpha a} C_{00} , \quad (\text{C.9})$$

$$a_2(d) = -\frac{1}{2} \tan \theta_W B^{i\alpha a*} B^{j\alpha b} \left[2C^{ab} C_{00} + \left(D^{ab} m_{\chi_a^0} m_{\chi_b^0} - C^{ab} m_{\tilde{l}_\alpha}^2 \right) C_0 - C^{ab} B_0 \right] , \quad (\text{C.10})$$

$$a_2(f) = \tan^2 \theta_W \sin^2 \theta_W B^{i\alpha a*} B^{j\alpha a} (B_0 + B_1) , \quad (\text{C.11})$$

Then we have

$$a_i = \frac{g_2}{2 \cos \theta_W} \frac{g_2^2}{16\pi^2} (a_i(b) + a_i(d)) , \quad i = 3, 4 \quad (\text{C.12})$$

and

$$a_3(b) = 2 \tan^2 \theta_W \left(\frac{1}{2} Z_L^{I\alpha} Z_L^{I\beta} - \sin^2 \theta_W \delta^{\alpha\beta} \right) B^{i\alpha a*} A^{j\beta a} m_{\chi_a^0} (C_0 + C_1 + C_2) , \quad (\text{C.13})$$

$$a_3(d) = \tan^2 \theta_W B^{i\alpha a*} A^{j\alpha b} (m_{\chi_b^0} C_1^{ab} + m_{\chi_a^0} D^{ab} C_2) , \quad (\text{C.14})$$

$$a_4(b) = 2 \tan^2 \theta_W \left(\frac{1}{2} Z_L^{I\alpha} Z_L^{I\beta} - \sin^2 \theta_W \delta^{\alpha\beta} \right) A^{i\alpha a*} B^{j\beta a} m_{\chi_a^0} (C_0 + C_1 + C_2) , \quad (\text{C.15})$$

$$a_4(d) = \tan^2 \theta_W A^{i\alpha a*} B^{j\alpha b} (m_{\chi_b^0} D^{ab} C_1 + m_{\chi_a^0} C^{ab} C_2) . \quad (\text{C.16})$$

All the coupling vertices A , B , C , D are defined in the Appendix B. The $B_{0,1}$ and $C_{0,1,2,00}$ are the standard two-point and three-point functions with its definition given in the program LoopTools [25]. The arguments of function B from Fig. (c), (d), (e), (f) are $(M_Z^2, m_{\chi_a^-}^2, m_{\chi_b^-}^2)$, $(M_Z^2, m_{\chi_a^0}^2, m_{\chi_b^0}^2)$, $(0, m_{\tilde{\nu}_\alpha}^2, m_{\chi_a^-}^2)$ and $(0, m_{\tilde{l}_\alpha}^2, m_{\chi_a^0}^2)$ respectively. The arguments of functions C from Figs. (a), (b), (c), (d) are $(0, M_Z^2, 0, m_{\chi_a^-}^2, m_{\tilde{\nu}_\alpha}^2, m_{\tilde{\nu}_\alpha}^2)$, $(0, M_Z^2, 0, m_{\chi_a^0}^2, m_{\tilde{l}_\alpha}^2, m_{\tilde{l}_\beta}^2)$, $(0, M_Z^2, 0, m_{\tilde{\nu}_\alpha}^2, m_{\chi_a^-}^2, m_{\chi_b^-}^2)$, $(0, M_Z^2, 0, m_{\tilde{l}_\alpha}^2, m_{\chi_a^0}^2, m_{\chi_b^0}^2)$ respectively, where the external fermion masses have been set to zero.

REFERENCES

- [1] Y. Fukuda et. al. , Phys. Rev. Lett. **82** (1999) 2644; Phys. Rev. Lett. **82** (1999) 5194; Phys. Lett. **B433** (1998) 9; Phys. Lett. **B436** (1998) 33; Phys. Lett. **B 467** (1999) 185.
- [2] T. Toshito, talk at the XXXth International Conference on High Energy Physics, July 27–August 2, 2000 (ICHEP 2000) Osaka, Japan (<http://ic hep2000.hep.sci.osaka-u.ac.jp>).
- [3] Y. Fukuda et. al. ,Phys. Rev. Lett. **81** (1998) 1562; Erratum **81**, (1998) 4279; Phys. Rev. Lett. **82** (1999) 2430; Y. Suzuki, Nucl. Phys. **B77**(Proc. Suppl.) (1999) 35.
- [4] T. Takeuchi, talk at the XXXth International Conference on High Energy Physics, July 27–August 2, 2000 (ICHEP 2000) Osaka, Japan (<http://ic hep2000.hep.sci.osaka-u.ac.jp>). M. C. Gonzalez-Garcia, these proceedings.
- [5] C. Athanassopoulos et al., Phys. Rev. Lett. **81** (1998) 1774; Phys. Rev. **C58** (1998) 2489.
- [6] S. M. Barr, hep-ph/0003058 and the references therein.
- [7] R. N. Mohapatra and G. Senjanović, Phys. Rev. Lett. **44** (1980) 912; see references in [6].
- [8] K.S. Babu, Jogesh C. Pati, Frank Wilczek, Nucl. Phys. **B566** (2000) 33; Jogesh C. Pati, Nucl. Phys. (Proc. Suppl.) 77 (1999) 299.
- [9] Jogesh C. Pati, hep-ph/0005095.
- [10] John Ellis, M. E. Gomez, G. K. Leontaris, S. Lola and D. V. Nanopoulos, Eur. Phys. J. **C14** (2000) 319 (hep-ph/9911459).
- [11] M. E. Gomez, G. K. Leontaris, S. Lola, J. D. Vergados, Phys. Rev. **D59** (1999) 116009

(hep-ph/9810291).

- [12] J. Hisano, Daisuke Nomura, Phys. Rev. **D59** (1999) 116005.
- [13] S. F. King and M. Oliveira, Phys. Rev. **D60** (1999) 035003.
- [14] Kiwoon Choi, Eung Jin Chun, Kyuwan Hwang, Phys. Lett. **B 488** (2000) 145; J. Hisano, Daisuke Nomura, Yasuhiro Okada, Yasuhiro Shimizu, Minoru Tanaka, Phys.Rev. **D 58** (1998) 116010; A. Ilakovac, Phys.Rev. **D 62** (2000) 036010; A. de Gouvea, S. Lola, K. Tobe, hep-ph/0008085.
- [15] C. H. Albright, S. M. Barr, hep-ph/0007145; hep-ph/0003251; Phys. Rev. Lett. **85** (2000) 244; Phys. Lett.
- [16] Guido Altarelli, Ferruccio Feruglio, hep-ph/9905536.
- [17] R. Hawking and K. Mönig, Eur. Phys. J. direct **C8** (1999) 1; J. I. Illana, T. Riemann, Nucl. Phys. (Proc Suppl) 89 (2000) 64; J. I. Illana, M. Jack and T. Riemann, hep-ph/0001273.
- [18] G. Mann and T. Riemann, Annalen Phys. **40** (1984) 334.
- [19] J. Rosiek, Phys. Rev. **D41** (1990) 3464.
- [20] V. Barger, M. S. Berger, P. Ohmann, Phys. Rev. **D49** (1994) 4908.
- [21] V. Barger, M. S. Berger, P. Ohmann, Phys. Rev. **D47** (1993) 1093; D. J. Castano, E. J. Piard, P. Ramond, Phys. Rev. **D49** (1994) 4882.
- [22] Hideo Fusaoka, Yoshio Koide, Phys. Rev. **D 57** (1998) 3986.
- [23] A subroutine which gives constraint on soft parameters in ISAJET is adopted in our calculations. See, for example, hep-ph/0001086 ,hep-ph/9810440.
- [24] Particle Data Group, Eur. Phys. J. C **15**, 1 (2000).

[25] T. Hahn, Acta Phys. Polon. **B30** (1999) 3469.

FIGURE CAPTIONS

FIG. 1 Feynman diagrams contributing to $\tau \rightarrow \mu\gamma$. The universal scalar neutrino masses become non-degenerate and mixed by the non-diagonal Yukawa couplings. This effect gives low energy scalar neutrino mixing by RGEs running.

FIG. 2 The Feynman diagrams contributing to the process $\tau \rightarrow \mu\gamma$.

FIG. 3 The Feynman diagrams contributing to the process $Z \rightarrow \mu\tau$. The other two self-energy diagrams coming from τ legs are omitted.

FIG. 4 Branching ratio of $\tau \rightarrow \mu\gamma$ as a function of m_0 for $m_{\frac{1}{2}} = 100\text{GeV}$, $\tan\beta = 5$ and $A_0 = 2m_0, m_0, 0$. The solid line is for $\mu > 0$ and the dashed line is for $\mu < 0$.

FIG. 5 Branching ratio of $\tau \rightarrow \mu\gamma$ as a function of m_0 for $A_0 = m_0$, $\tan\beta = 5$ and $m_{\frac{1}{2}} = 100\text{GeV}, 200\text{GeV}, 400\text{GeV}$. The solid line is for $\mu > 0$ and the dashed line is for $\mu < 0$.

FIG. 6 Branching ratio of $\tau \rightarrow \mu\gamma$ as a function of m_0 for $m_{\frac{1}{2}} = 100\text{GeV}$, $\tan\beta = 10$, $\mu > 0$ and $A_0 = \pm 2m_0, \pm m_0, 0$. The solid line is for $A_0 > 0$ and the dashed line is for $A_0 < 0$.

FIG. 7 Branching ratio of $\tau \rightarrow \mu\gamma$ as a function of m_0 for $A_0 = m_0$, $m_{\frac{1}{2}} = 100\text{GeV}$, and $\tan\beta = 2, 5, 10$. The solid line is for $\mu > 0$ and the dashed line is for $\mu < 0$.

FIG. 8 Branching ratio of $Z \rightarrow \mu\tau$ as a function of m_0 for $m_{\frac{1}{2}} = 100\text{GeV}$, $\tan\beta = 5$ and $A_0 = 2m_0, m_0, 0$. The solid line is for $\mu > 0$ and the dashed line is for $\mu < 0$.

FIG. 9 Branching ratio of $Z \rightarrow \mu\tau$ as a function of m_0 for $A_0 = 2m_0$, $\tan\beta = 5$ and $m_{\frac{1}{2}} = 100\text{GeV}, 200\text{GeV}, 400\text{GeV}$. The solid line is for $\mu > 0$ and the dashed line is for $\mu < 0$.

FIG. 10 Branching ratio of $Z \rightarrow \mu\tau$ as a function of m_0 for $A_0 = 2.5m_0$, $m_{\frac{1}{2}} = 150\text{GeV}$, and $\tan\beta = 2, 5, 10$.

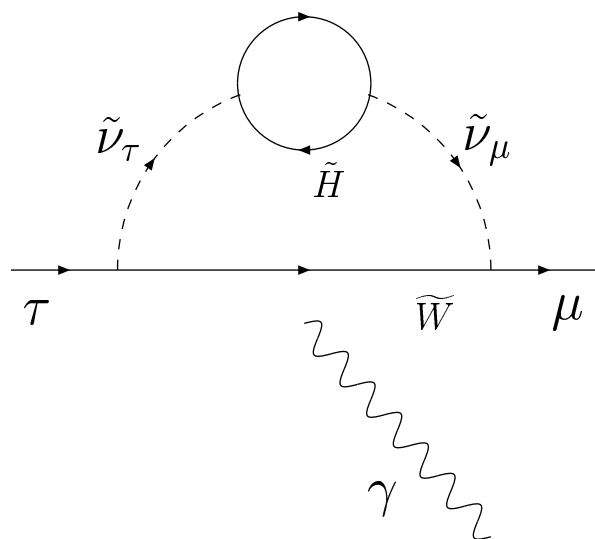


Fig. 1

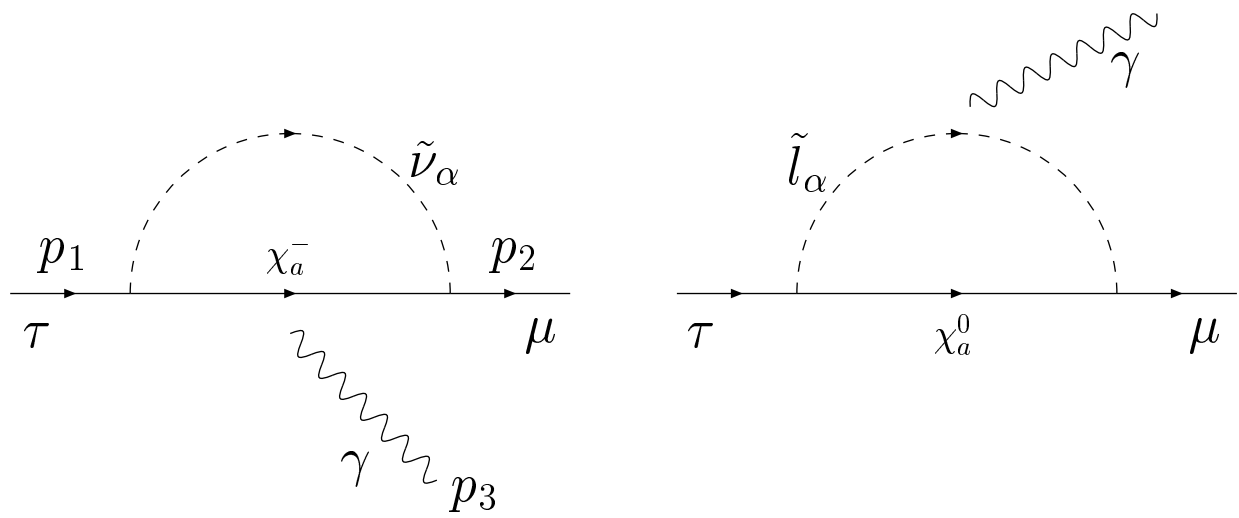


Fig. 2

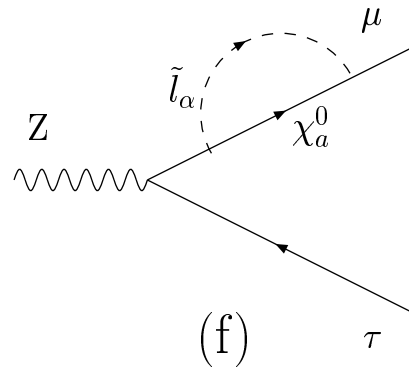
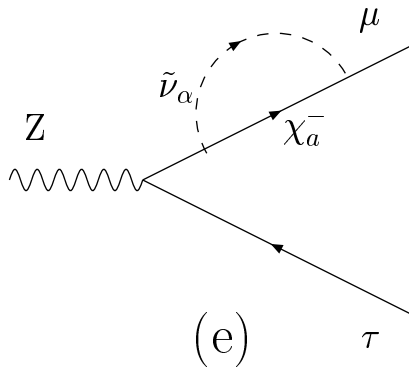
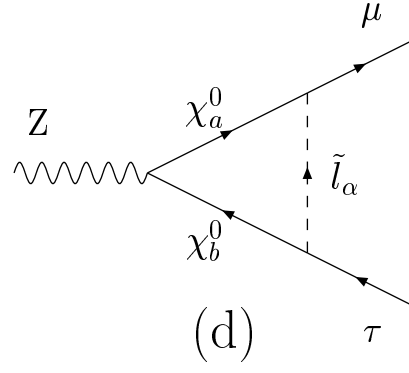
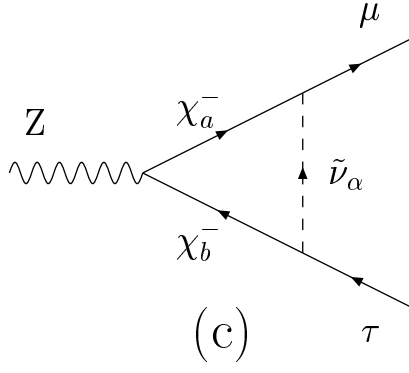
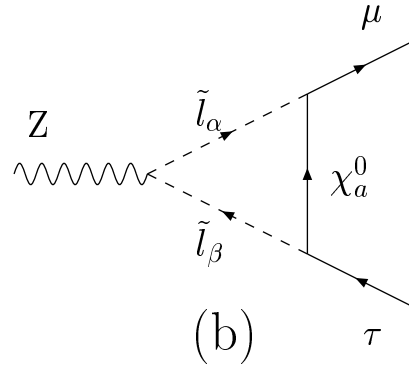
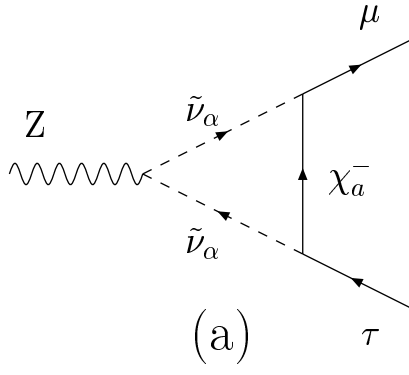


Fig. 3

Fig. 4

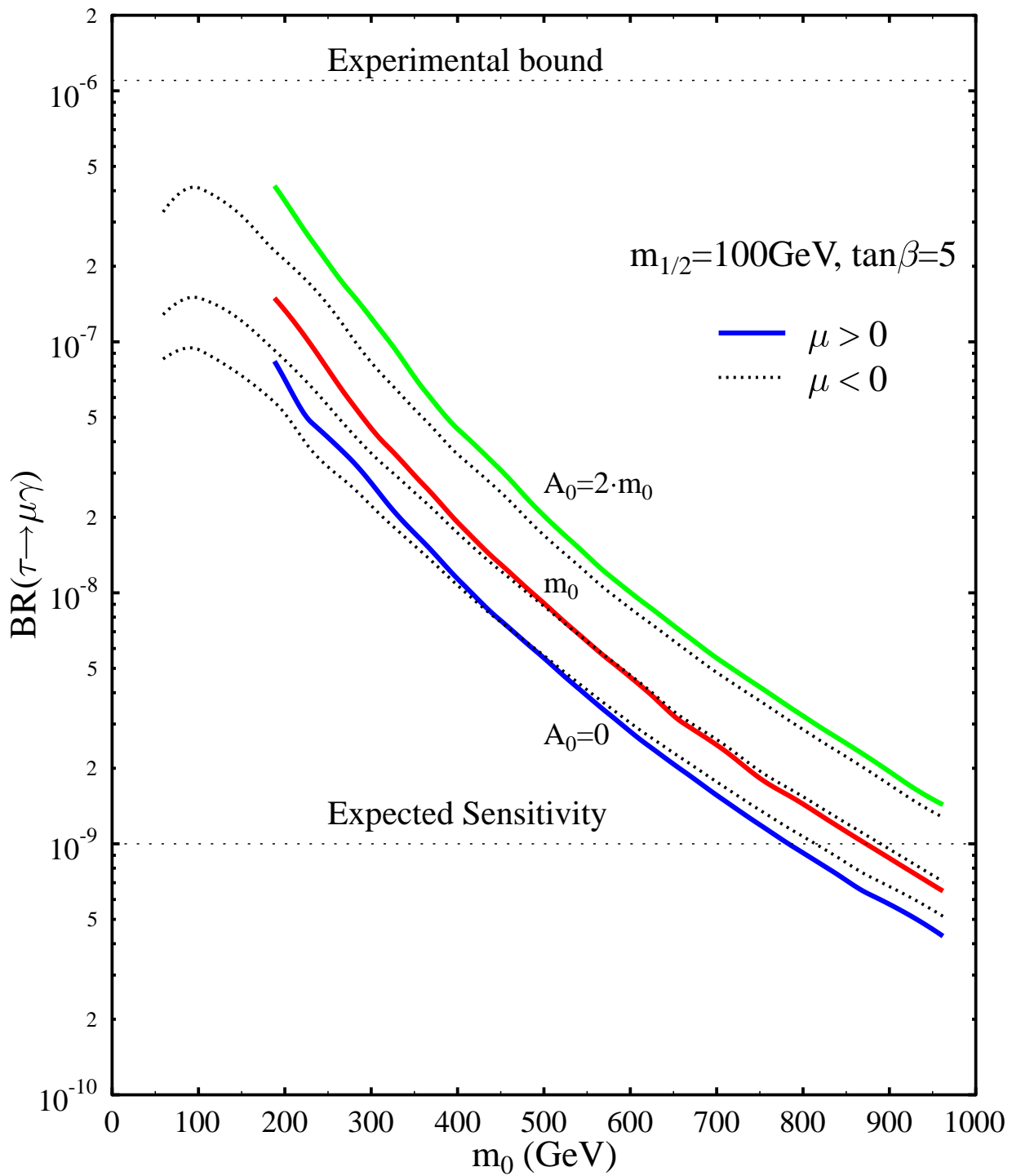


Fig. 5

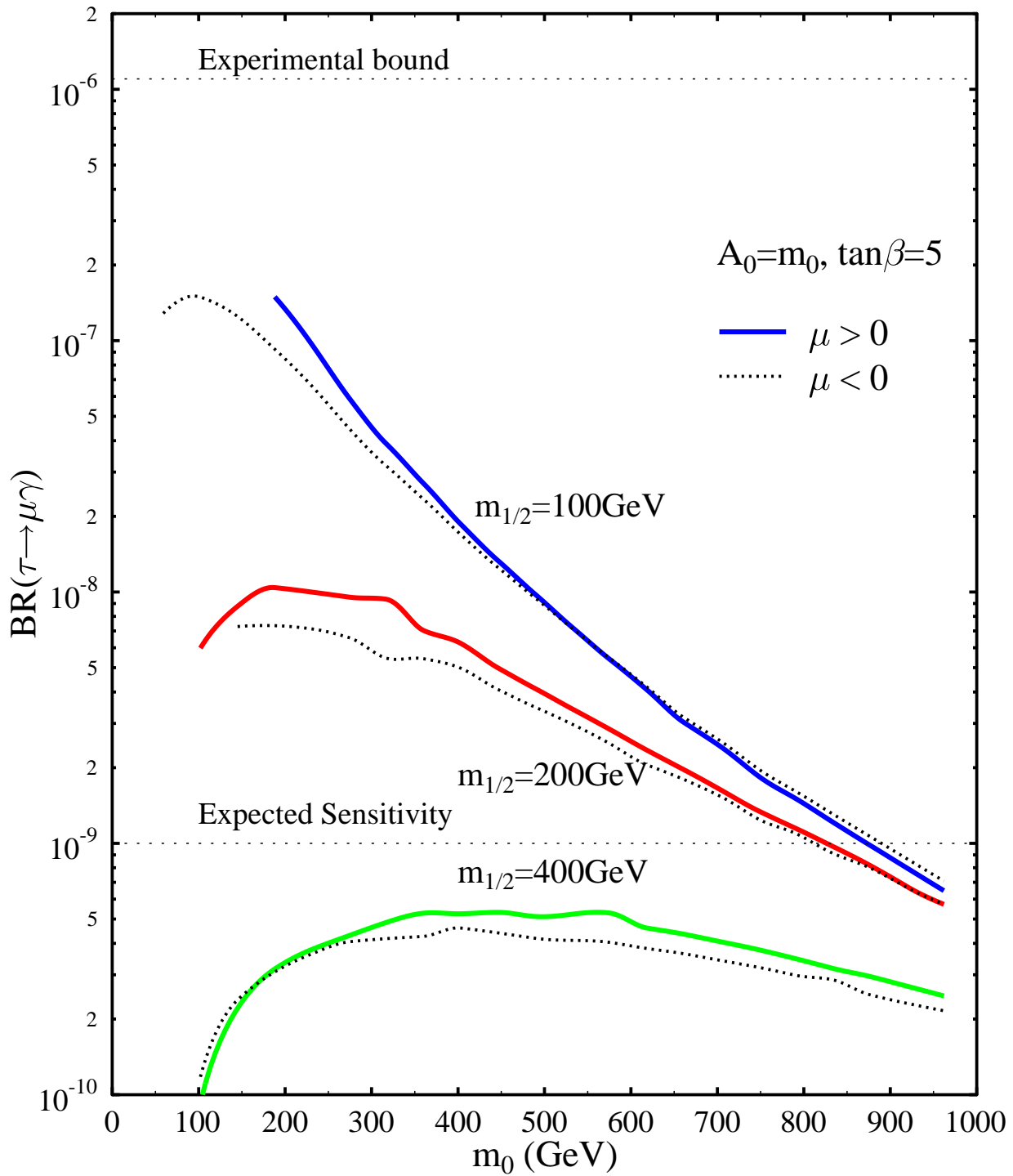


Fig. 6

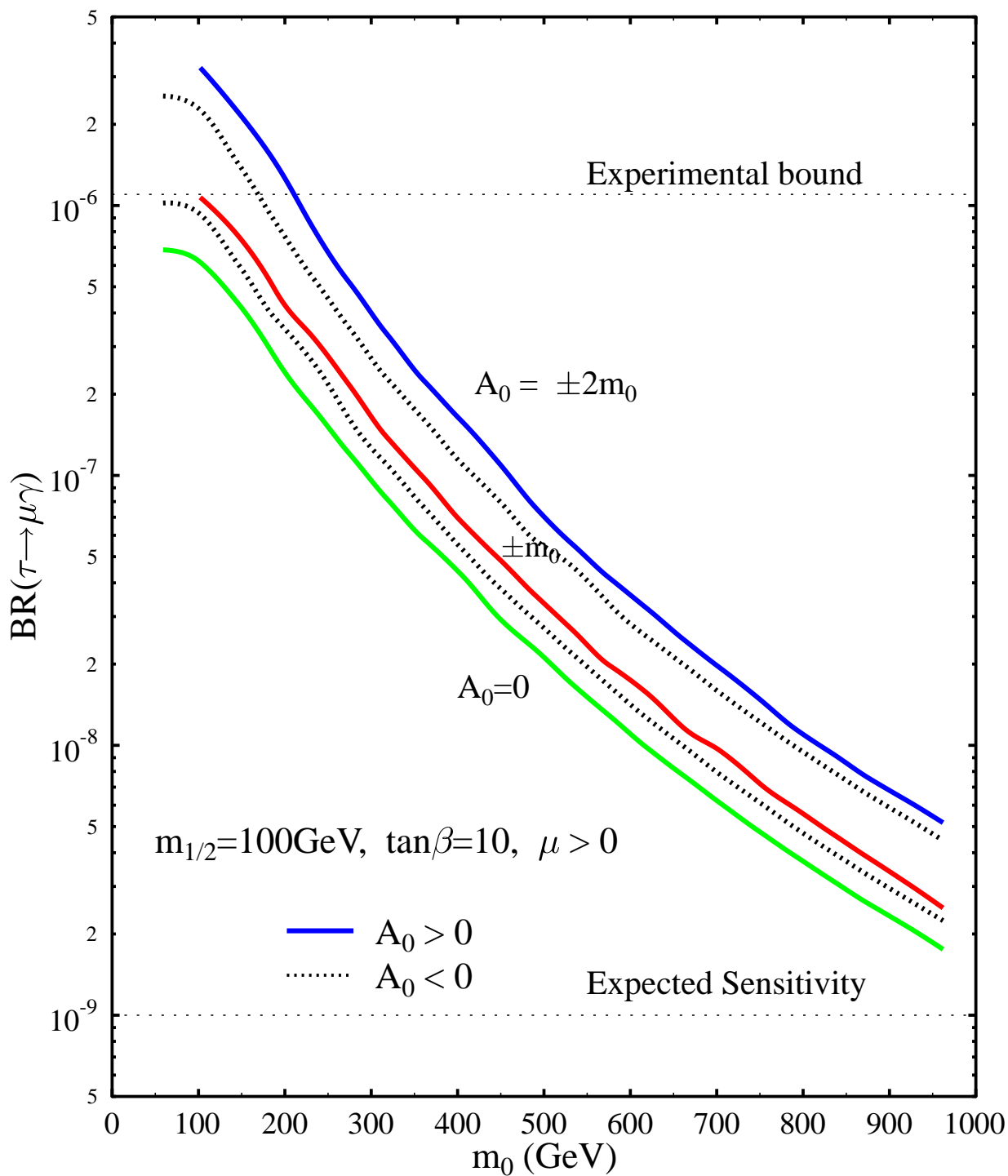


Fig. 7

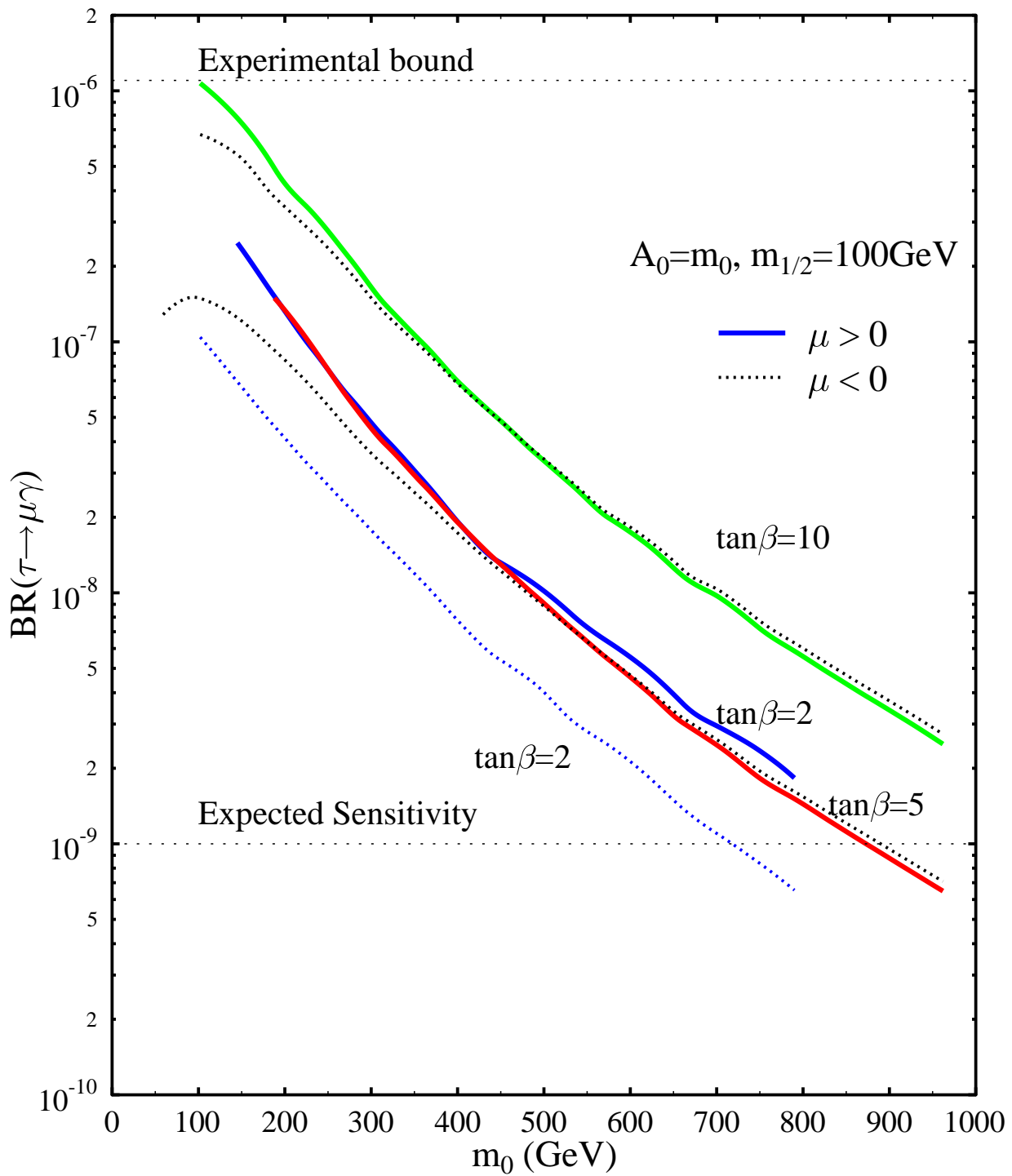


Fig. 8

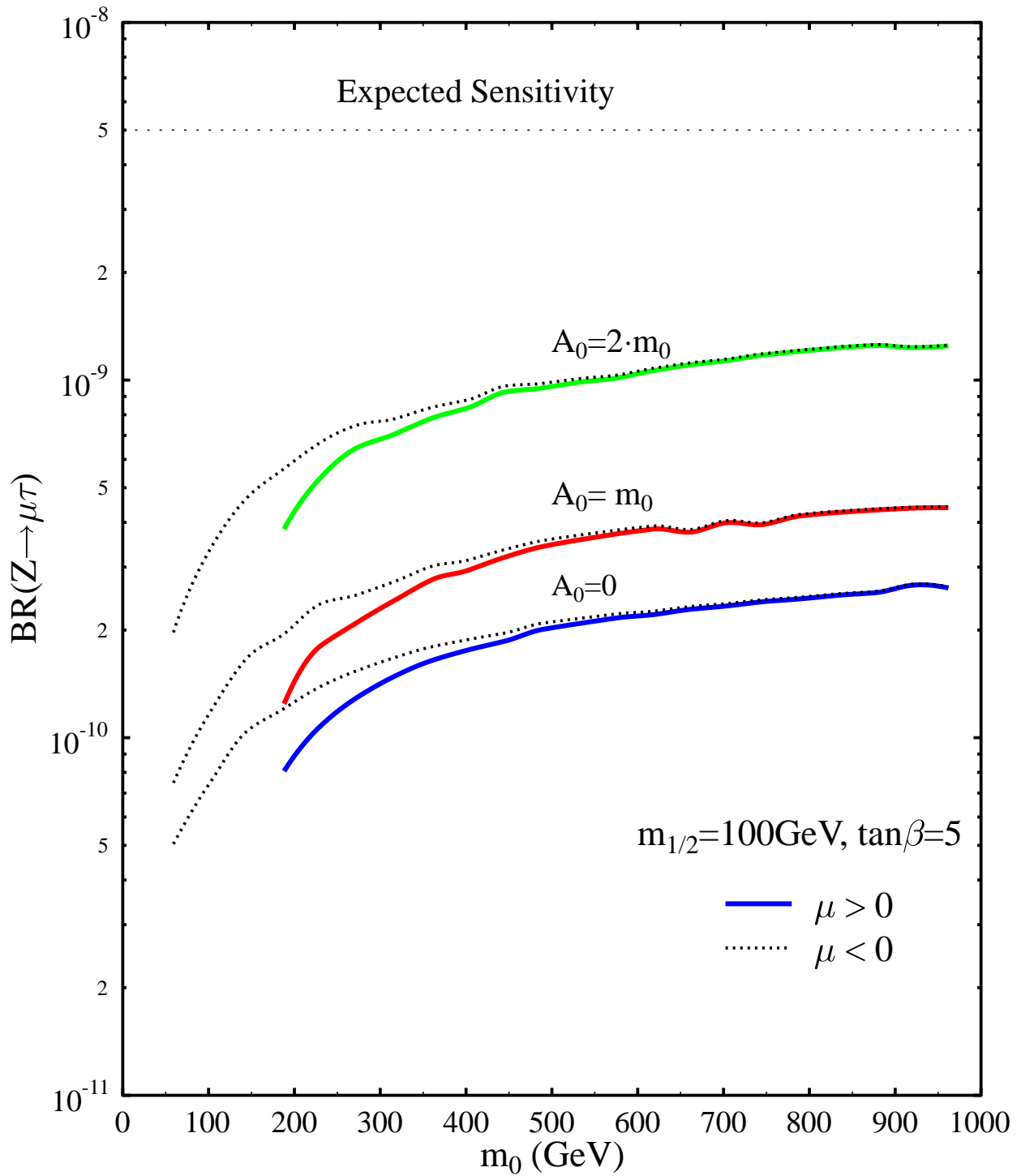


Fig. 9

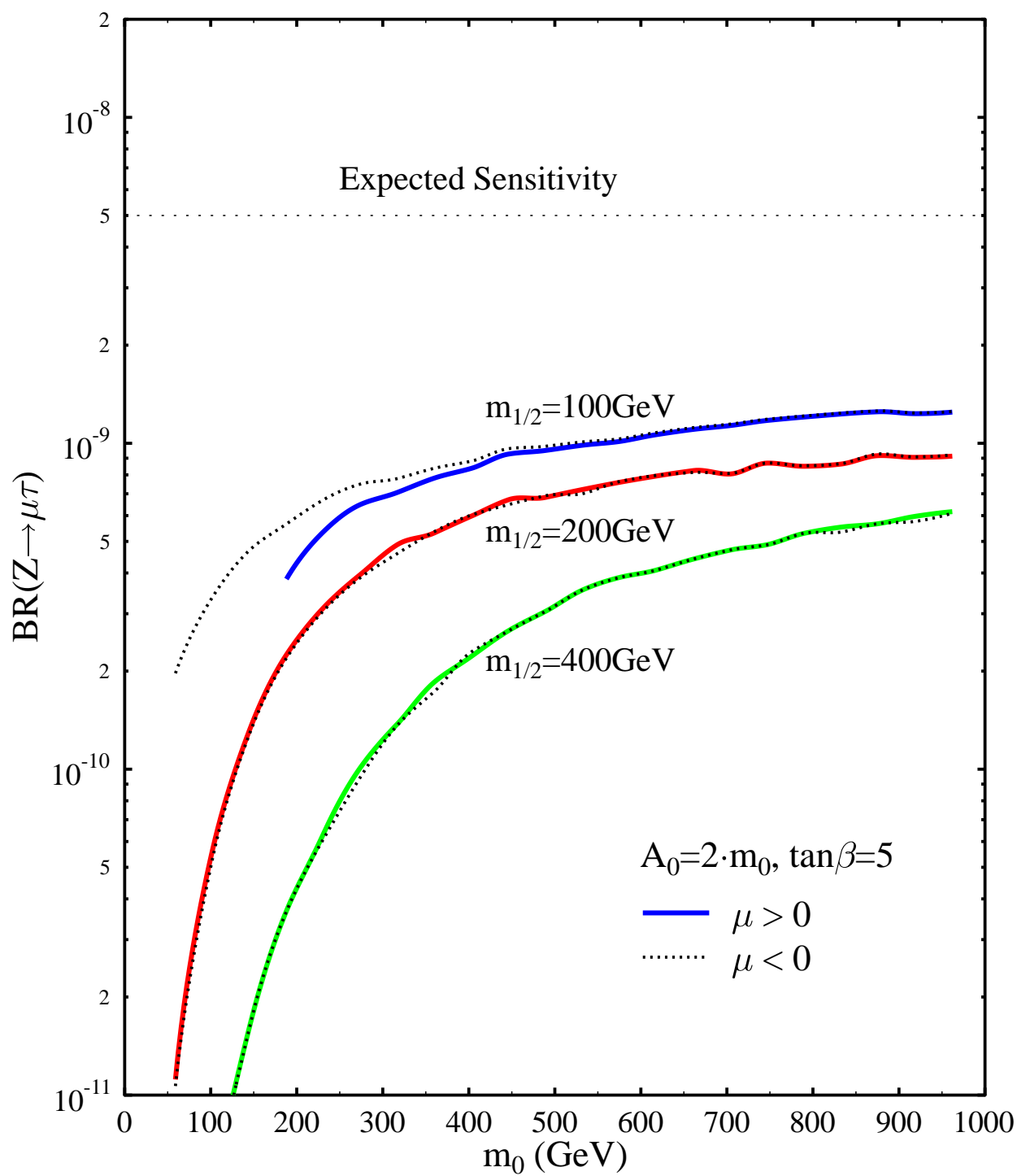


Fig. 10

